

The role of the pseudogap in cuprate superconductors demonstrated by the Hall effect

Júlia C. Anjos, Hércules Santana and E. V. L. de Mello¹

¹*Instituto de Física, Universidade Federal Fluminense, 24210-346 Niterói, RJ, Brazil**

Cuprate high-temperature superconductors are known to have a normal-state pseudogap but, after many years of intense research, its relation to the superconductivity is still a mystery. Similarly, the in-plane Hall coefficient R_H has a large temperature variation caused by changes in the carrier density which is also a long-standing puzzle. We approach both problem by a kinetic theory of phase separation that reproduces the charge density wave by a free energy array of potential wells. The charge modulation favors local hole-hole attraction yielding local superconducting pairs and a transition by long-range phase order at T_c . As the temperature increases the modulations decrease and the charge density increases by thermal activation. This approach reproduces the R_H of $\text{La}_{2-x}\text{Sr}_x\text{CuO}_4$ compounds of $x = 0.0 - 0.25$ and clarifies the role of the pseudogap and the disorder in cuprates.

The underlying physics of the pseudogap has long been probed by many different experiments and techniques¹ but it is still shrouded in mystery². It is observed in both electron and hole-doped cuprate, but remains unresolved despite many years of intense studies³. More concerning still, there is not an agreement on the precise phase boundaries and phenomenology of this normal state gap. It is agreed that it represents a partial gap in the electronic density of states⁴ and is seen in the antinodal region of k -space⁵. Once, it was believed to be solely associated with the under-doped side of the phase diagram but now it is described as a line falling to zero either at a critical doping in the overdoped region^{4,6} or at the end of the superconducting dome^{4,7}.

On the other hand, the in-plane Hall coefficient $R_H = 1/ne$, where e is the electron charge and n the itinerant carrier density, probes the charge dynamics of metals and semiconductors⁸. In metals described by the Fermi liquid model, R_H is constant and negative because the conduction band density of electrons. In cuprate high-temperature superconductors (HTS), it is positive due to the hole carriers and has a large variation with the temperature. Comparison between powder and single crystals data demonstrated that the magnitude and temperature dependence of R_H is dominated by the in-plane contribution⁹ but after all these years there is not an explanation why n varies with the temperature.

We propose here that R_H is influenced by the planar charge instabilities that is observed in different forms like stripes¹⁰, checkerboard¹¹ or puddles¹². At first, this was a phenomenon attributed solely to weakly doped compounds around $p = 1/8$ per Cu atom, where the charge density wave (CDW) signal is generally more intense¹³⁻¹⁵. However, a variety of complementary experimental probes have detected charge instability in all hole-doped HTS families¹⁶ as well as in Nd-based electron-doped¹⁷. More recently, CDW has been detected in overdoped $\text{La}_{2-x}\text{Sr}_x\text{CuO}_4$ (LSCO) up to at least $p \equiv x = 0.21$ ¹⁸⁻²¹ and possibly up to $p = 0.27$ in the form of puddles^{22,23}. This overall presence of various forms of incommensurate charge order (CO) suggests that they may be more intimately related with the superconducting phase than initially thought.

Accordingly, we have developed a model which the pseudogap is a mesoscopic electronic phase separation that leads to CO in HTS is precursor of the superconductivity²⁴⁻²⁹.

We study this phenomenon by the time-dependent non-linear Cahn–Hilliard (CH) differential equation used to describe the order-disorder transition of binary alloys formation. The method minimizes a Ginzburg–Landau (GL) free energy given by the (phase separation) order parameter power expansion^{24,25}. The GL potential (V_{GL}) forms an array of wells hosting alternate high and low hole densities domains of wavelength λ_{CO} size (see Fig.1). The low density regions favor antiferromagnetic (AF) fluctuations that are reminiscent of the Mott AF ground state of low doping compounds and whose existence was central to several magnetic mediated pairing theories^{2,4}. When T approaches $T^*(p)$, the V_{GL} amplitude or modulation decreases untightening the CO, what makes, for instance, the softening of the x-ray peaks^{14,15} and the angle-resolved photoemission spectroscopy (ARPES)^{7,30}. We take this effect in $R_H(p, T)$ by calculating the flow of holes tunnelling through the nanoscopic barriers shown in Fig. 1 and insets.

The presence of $T^*(p)$ and the similarities between CO in hole- and electron-doped phase diagrams¹⁷ suggest the existence of CDW modulations also around the half-filled ($p = 0$ or $n = 1$). In other words, even the insulator compounds with $n \approx 1$ possess the V_{GL} or charge modulations. Indeed, the variations of $R_H(p, T)$ at high temperatures³¹ in compounds with very low p support this statement. Therefore, in samples with larger doping, the additional p holes tend to fill in alternating high and low-density domains. Then, in a typical compound with $n = 1 + p$ itinerant carriers, the half-filled $n = 1$ are associated with the V_{GL} free energy potential and p become localized in the CDW domains in agreement with a coexisting two-gap or two-particle scenario verified by different experiments^{4,5,32,33}.

In this scenario, the tunnelling process through the array of V_{GL} and the two well-known energies of pseudogap and superconducting gap^{4,5,32,33} are sufficient to interpret the dynamics of the holes as a function of temperature. Expressing these two energies as proportional to $T^*(p)$ and the onset of pair formation $T_c^{\text{max}}(p)$, we reproduce the main aspects of the temperature and doping dependence of $R_H(p, T)$ of LSCO^{9,31,34,35}. These Hall effect calculations with these two aspects of the charges provide knowledge to understand the basic building blocks of HTS, notably the role of the pseudogap.

The calculations start with the time-dependent CH equation which reproduces the CDW charge instability. It is written in terms of the local phase separation order parameter $u(r_i, t) = (p(r_i, t) - p)/p$, where $p(r_i, t)$ is the local charge or hole density at a unit cell position i in the CuO plane and p is the average doping level^{26–28,36,37}. The simulation evolves to total phase separation, but it is stopped when the charges reach a configuration close to a given CO with the λ_{CO} of a sample. The CH equation is based on minimizing the GL free energy:^{25,26,38}

$$f(u) = \frac{1}{2}\varepsilon|\nabla u|^2 + V_{GL}(u, T), \quad (1)$$

where ε is the parameter that controls the charge modulations λ_{CO} and $V_{GL}(u, T) = -A^2u^2/2 + B^2u^4/4 + \dots$ is a double-well potential. The charge oscillations appear below the phase separation temperature T_{PS} , $B = 1$ and $A^2 = \alpha(p)[T_{PS} - T]$. In Fig. 1 we show a typical low temperature $V_{GL}(u(r_i, T))$ simulation and its valleys which tend to bound the carriers in alternating high and low densities CDW domains. We show in the inset (a), the $V_{GL}(u(r_i, T))$ amplitude along the x -direction that diminishes when the temperature raises towards $T_{PS} \geq T^*$ where the system becomes homogeneous. The size of the barriers between the two (high and low charge density) phases is proportional to A^4/B^2 or $\langle V_{GL}(p, T) \rangle = \alpha(p)^2[T^* - T]^2$, for $T \leq T^*$.

Thus, at low temperatures, V_{GL} produces alternating high and low charge domains and such inhomogeneous carrier distribution induces ions' fluctuations that may lead to hole-hole attraction^{27,36}. Such indirect interaction yields local superconducting pairs proportional to the barrier size $\langle V_{GL}(p, T) \rangle$ what is in agreement with the HTS coherence lengths being smaller than the CO wavelength^{25,26,28}, i.e., $\xi_{sc} \leq \lambda_{CO}$. On the other side, when the temperature increases, $V_{GL}(p, T)$ diminishes as shown in inset (a) and the carriers become uniform which leads to the temperature effect on $R_H(p, T)$ that we will detail below.

We mentioned before that the $p = 0$ Hall measurements³¹ also display an increase in the number of hole carriers with the temperature similar to most of the compounds, up to the overdoped side. This behavior indicates that possibly all the samples undergo a continuous phase separation below $T \approx T^*$. At low temperatures, $V_{GL}(p, T)$ has a series of ‘‘ice cream cones’’ as shown in Fig. 1 which slowly ‘‘melts’’ when the temperature raises. For $p \geq 0.0$, at low temperatures, the p doping holes tend to become localized or even trapped in the $n = 1$ CDW domains, where they may also form local pairs^{28,36,37}. According to this scenario, we distinguish three independent temperature dependence to $R_H(p, T)$;

First, the two sources of carriers mentioned above:

i- The p holes of a $n = 1 + p$ compound become localized in the CDW alternating charge domains and, eventually, at low temperatures they form local superconducting order parameter that establish local amplitudes and the superconducting state by phase coherence²⁴. The energy of these pairs are not scaled by T_c but by T_c^{max} , that is, the onset of experimental superconducting pairs or precursor pairs

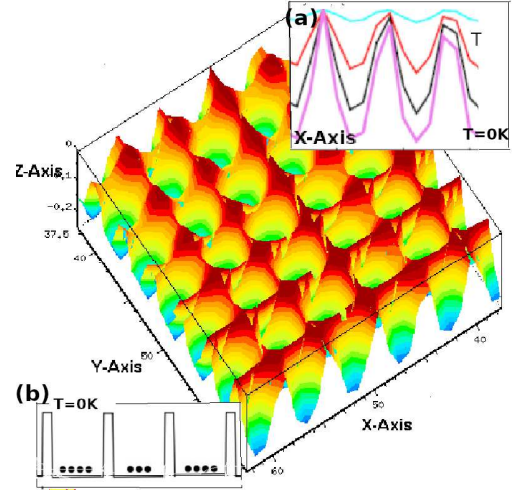


FIG. 1. Low-temperature CH simulations of the planar GL free energy phase separation potential with its valleys and barriers that originate the CDW structure. Inset (a) shows the V_{GL} profile along the x -direction for increasing T up to near T^* . In the inset (b) we describe the simplified model to the $T = 0$ K potential barriers to the transmission coefficient used to calculate the number of carriers with the temperature.

detected by many experiments like ARPES³⁰ and STM³⁹. Below T_c^{max} the localized superconducting pairs form an array of mesoscopic Josephson junctions, and R_H is small. As the temperatures increases above T_c but below T^* , these pairs eventually brake free and R_H has a maximum near T_c^{max} . The number of unbound holes is obtained by thermal excitation; $n_1(p, T) = pB_c(1 + \exp(-T_c^{max}/T))$, where $B_c = 2$ is the number of CuO planes in the unit cell of LSCO⁴⁰.

ii- The $R_H(p, T)$ variation with the temperature³¹ indicates that the CDW free energy modulations are already present at half-filled ($n = 1.0$ and $p = 0$). Therefore we assume that such modulations are formed by the half-filled holes and not by the hole density (p) from doping. Again, with the rise in temperature, the modulations of V_{GL} decrease as shown in the inset (a) of Fig. 1 because part of these $n = 1.0$ holes diffuse through the system. Since the CDW sets in at T^* this process is scaled by the pseudogap temperature and the temperature dependence of the number density of such carriers is given by thermal activation; $n_2(p, T) = nB_c(1 + \exp(-T^*(p)/T))$, where $n = 1$ is the same to all compounds from $p = 0$ to $p = 0.25$.

iii- Furthermore, all carriers have to move through the background of the $V_{GL}(p, T)$ modulations that are large at low doping and low temperatures but decrease when the system is warmed, as shown in the inset (a) of Fig. 1. This is taken into account by the tunnelling current probability between the charge domains which is not easy to calculate exactly, and we adopted a simplified model based on one-dimensional quantum mechanics transmission coefficient⁴¹. In this way, the tunnelling expression through rectangular barriers like those

shown in the inset (b) of Fig. 1 with width of $\lambda_{\text{CO}}/2$ and height proportional to $\langle V_{\text{GL}}(p, T) \rangle$ is given by.

$$T_{\text{trans}}^2 = n(p, T) e^{-[\gamma \langle V_{\text{GL}} \rangle (1 - (T/T^*)^2)^{1/2}]^2} \quad (2)$$

where $n(p, T) = n_1(p, T) + n_2(p, T)$ is the total number density of holes, $n_1(p, T)$ and $n_2(p, T)$ are given just above, $\gamma = 2m\hbar^2/\lambda_{\text{CO}}^2$ and m is the electron mass. The values of $\langle V_{\text{GL}} \rangle$ have been calculated before in Refs. 27 and 28 and the ones used in the calculations are listed in Table I. Notice that $\gamma \langle V_{\text{GL}} \rangle$ is adimensional and a measurement of the CDW roughness.

Now we use the above calculated $n(p, T)$ to reproduce the temperature dependence of the number of holes that is the main and most puzzling ingredient of $R_{\text{H}}(p, T)$. These very simple expressions are robust enough to describe all $p \leq 0.25$ experimental values^{9,31,34,35} using only their values of $T^*(p)$ and $T_c^{\text{max}}(p)$. For $0.0 < p \leq 0.05$ we keep the $n(p, T)$ constant for $T \leq T_{\text{AF}} = 300$ K, the Neel temperature, because the antiferromagnetic phase. The low density AF clusters act like as if the carriers are frozen what yields a plateau³¹ in $R_{\text{H}}(p, T)$.

The values of $\langle V_{\text{GL}} \rangle' = 2m\hbar^2/\lambda_{\text{CO}}^2 \langle V_{\text{GL}} \rangle = \gamma \langle V_{\text{GL}} \rangle$ for under and overdoped LSCO are obtained from the tables in the supplemental information of Ref. 27 and $\lambda_{\text{CO}}^2(p)$ from Ref. 16. For instance, the optimal doped $p = 0.16$ has²⁷ $\langle V_{\text{GL}} \rangle' = 0.234$ meV and $\lambda_{\text{CO}} = 3.9a_0$ with $a_0 = 3.78\text{\AA}$ and $\sqrt{\gamma \langle V_{\text{GL}} \rangle'} = 1.833$, and therefore we use in Eq. 2 the value 1.80 to $p = 0.15$. $\langle V_{\text{GL}} \rangle'$ to other p 's are either calculated in this way or, like the small doping compounds that we do not have all the data, are extrapolated. We list these results in the last column of the Table I below.

The $R_{\text{H}}(p, T)$ results from the above analysis are shown in Fig. 2 with the experimental data of Ref. 31 and the agreement is very good from $p = 0.0$ to 0.23. Only $p = 0.25$ diverges from our calculations above $T = 100$ K. The decrease of the experimental $R_{\text{H}}(p, T)$ is most likely due to the negative Hall coefficient of out-of-plane electrons of strong overdoped samples that was reported by Ref. 35. The presence of electrons may be connected with the decrease of the roughness parameter below 1.0 shown in Table I.

In conclusion, the pseudogap's role in cuprate superconductors as a mediator of phase separation and the two-particle and two-gap scenario⁴ are identified by the $R_{\text{H}}(p, T)$ calculations. The model based on phase-ordering kinetics²⁷ reveal the nature of the two types of carriers in a typical compound of $n = 1 + p$ hole doping: The half-filled charges ($n = 1$) of a single band are responsible by the phase separation free energy shown in Fig. 1 and scaled by the temperature $T^*(p)$. The other p holes of a $n = 1 + p$ compound fill in the alternating CDW domains breaking the uniform charge distribution and inducing ion-mediated pair interaction. The energy of these pairs are scaled by the onset temperature of superconducting pair formation^{30,39} $T_c^{\text{max}}(p)$, that is just a few times T_c (see Table I). For low doping the physical properties like superfluid density or quantum oscillations^{6,37} are dominated by the thermal activated $n = p$ holes because $T_c^{\text{max}}(p) \ll T^*(p)$. Increasing doping, above $p \approx 0.19$ the two energies or temperatures converge to the same order of magnitude¹⁹ (see Ta-

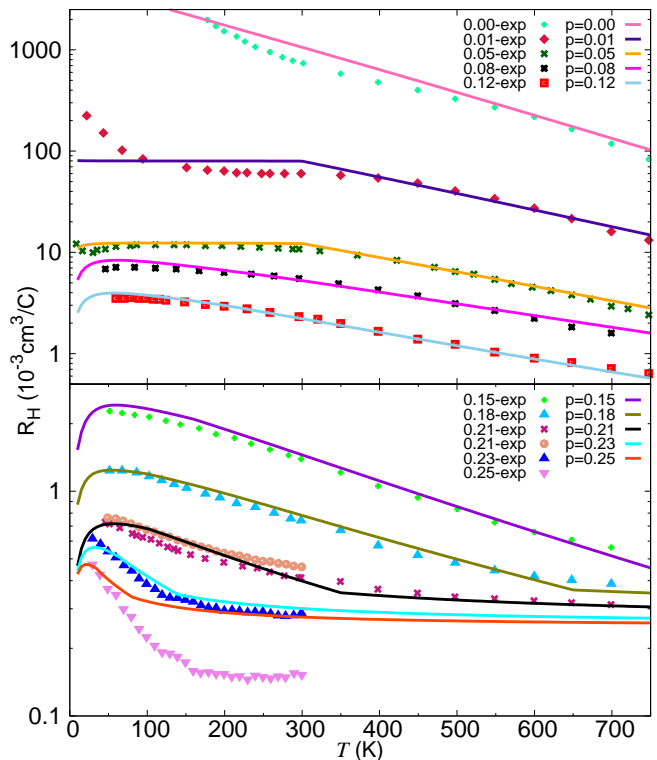


FIG. 2. The $R_{\text{H}}(p, T)$ experimental points from Ref. 31 and $p = 0.21$ from Ref. 34 with the theoretical model derived in the text (the continuous lines). The agreement is good from $p = 0.0$ to 0.23. The case of $p = 0.25$ is the only one yielding much larger values above $T = 100$ K, what is most likely due to the negative $R_{\text{H}}(p, T)$ of out-of-plane electrons in strong overdoped samples according to Ref. 35.

TABLE I. Properties of LSCO used in the calculations. The first column is hole doping density per unit cell. Second is the T^* and third is T_c that does not enter in the calculations but is a good reference and the last column is the renormalized free energy barrier $\sqrt{\langle V_{\text{GL}} \rangle'}$ or roughness factor explained in the text.

Sample	T^* (K)	T_c (K)	T_c^{max} (K)	$\sqrt{\langle V_{\text{GL}} \rangle'}$
$p = 0.00$	1800	0.0	0.0	9.0
$p = 0.01$	1700	0.0	10.0	6.0
$p = 0.05$	1350	1.0	70.0	4.0
$p = 0.08$	1300	20.0	280.0	3.0
$p = 0.12$	900	34.0	200.0	2.3
$p = 0.15$	850	39.0	160.0	1.8
$p = 0.18$	650	36.0	160.0	1.1
$p = 0.21$	350	24.0	110.0	0.6
$p = 0.23$	140	18.0	70.0	0.4
$p = 0.25$	80	12.0	40.0	0.2

ble I) and the carrier concentration detected in experiments crosses over from p to $1 + p$ ^{6,22,23,37}. Taking into account the above temperature dependent contributions we reproduced *all* the LSCO $R_{\text{H}}(p, T)$ measurements.

We acknowledge partial support from the Brazilian agen-

- * Corresponding author: evlmello@id.uff.br
- ¹ T. Timusk and B. Statt, Reports on Progress in Physics **62**, 61 (1999).
 - ² D. P. M. R. Norman and C. Kallin, Advances in Physics **54**, 715 (2005).
 - ³ A. A. Kordyuk, Low Temperature Physics **41**, 319 (2015).
 - ⁴ S. Hüfner, M. A. Hossain, A. Damascelli, and G. A. Sawatzky, Reports on Progress in Physics **71**, 062501 (2008).
 - ⁵ W. D. Wise, M. C. Boyer, K. Chatterjee, T. Kondo, T. Takeuchi, H. Ikuta, Y. Wang, and E. W. Hudson, Nature Physics **4**, 696 (2008).
 - ⁶ S. Badoux, W. Tabis, F. Laliberté, G. Grissonnanche, B. Vignolle, D. Vignolles, J. Béard, D. A. Bonn, W. N. Hardy, R. Liang, N. Doiron-Leyraud, L. Taillefer, and C. Proust, Nature **531**, 210 (2016).
 - ⁷ M. Hashimoto, I. M. Vishik, R.-H. He, T. P. Devereaux, and Z.-X. Shen, Nature Physics **10**, 483 (2014).
 - ⁸ N. P. Ong, “Physical properties of high temperature superconductors ii,” (World Scientific, Singapore, 1990).
 - ⁹ H. Y. Hwang, B. Batlogg, H. Takagi, H. L. Kao, J. Kwo, R. J. Cava, J. J. Krajewski, and W. F. Peck, Phys. Rev. Lett. **72**, 2636 (1994).
 - ¹⁰ J. M. Tranquada, B. J. Sternlieb, J. D. Axe, Y. Nakamura, and S. Uchida, Nature **375**, 561 (1995).
 - ¹¹ T. Hanaguri, C. Lupien, Y. Kohsaka, D.-H. Lee, M. Azuma, M. Takano, and J. C. Takagi, H. and Davis, Nature **430**, 1001 (2004).
 - ¹² K. M. Lang, V. Madhavan, J. E. Hoffman, E. W. Hudson, H. Eisaki, S. Uchida, and J. C. Davis, Nature **415**, 412 (2002).
 - ¹³ G. Ghiringhelli, M. Le Tacon, M. Minola, S. Blanco-Canosa, C. Mazzoli, N. B. Brookes, G. M. De Luca, A. Frano, D. G. Hawthorn, F. He, T. Loew, M. Moretti Sala, D. C. Peets, M. Salluzzo, E. Schierle, R. Sutarto, G. A. Sawatzky, E. Weschke, B. Keimer, and L. Braicovich, Science (New York, N.Y.) **337**, 821 (2012).
 - ¹⁴ M. Hücker, N. B. Christensen, A. T. Holmes, E. Blackburn, E. M. Forgan, R. Liang, D. A. Bonn, W. N. Hardy, O. Gutowski, M. V. Zimmermann, S. M. Hayden, and J. Chang, Physical Review B **90**, 1 (2014).
 - ¹⁵ S. Blanco-Canosa *et al.*, Physical Review B **90**, 054513 (2014).
 - ¹⁶ R. Comin and A. Damascelli, Ann. Rev. of Cond. Mat. Phys. **7**, 369 (2016).
 - ¹⁷ E. H. da Silva Neto, M. Minola, B. Yu, W. Tabis, M. Bluschke, D. Unruh, H. Suzuki, Y. Li, G. Yu, D. Betto, K. Kummer, F. Yakhou, N. B. Brookes, M. Le Tacon, M. Greven, B. Keimer, and A. Damascelli, Phys. Rev. B **98**, 161114 (2018).
 - ¹⁸ J. Wu, A. T. Bollinger, X. He, and I. Božović, Nature **547**, 432 (2017).
 - ¹⁹ S.-D. Chen, M. Hashimoto, Y. He, D. Song, K.-J. Xu, J.-F. He, T. P. Devereaux, H. Eisaki, D.-H. Lu, J. Zaanen, and Z.-X. Shen, Science **366**, 1099 (2019).
 - ²⁰ Y. Fei, Y. Zheng, K. Bu, W. Zhang, Y. Ding, X. Zhou, and Y. Yin, Science China Physics, Mechanics & Astronomy **63**, 227411 (2019).
 - ²¹ H. Miao, G. Fabbris, R. J. Koch, D. G. Mazzone, C. S. Nelson, R. Acevedo-Esteves, G. D. Gu, Y. Li, T. Yilimaz, K. Kaznatcheev, E. Vescovo, M. Oda, T. Kurosawa, N. Momono, T. Assefa, I. K. Robinson, E. S. Bozin, J. M. Tranquada, P. D. Johnson, and M. P. M. Dean, npj Quantum Materials **6**, 31 (2021).
 - ²² Y. Li, A. Sapkota, P. M. Lozano, Z. Du, H. Li, Z. Wu, A. K. Kundu, R. J. Koch, L. Wu, B. L. Winn, S. Chi, M. Matsuda, M. Frontzek, E. S. Božin, Y. Zhu, I. Božović, A. N. Pasupathy, I. K. Drozdov, K. Fujita, G. D. Gu, I. A. Zaliznyak, Q. Li, and J. M. Tranquada, Phys. Rev. B **106**, 224515 (2022).
 - ²³ W. O. Tromp, T. Benschop, J.-F. Ge, I. Battisti, K. M. Bastiaans, D. Chatzopoulos, A. H. M. Vervloet, S. Smit, E. van Heumen, M. S. Golden, Y. Huang, T. Kondo, T. Takeuchi, Y. Yin, J. E. Hoffman, M. A. Sulangi, J. Zaanen, and M. P. Allan, Nature Materials **22**, 703 (2023).
 - ²⁴ E. V. L. de Mello, Europhys. Lett. **99**, 37003 (2012).
 - ²⁵ E. V. L. deMello and J. E. Sonier, J. Phys.: Condens. Matter **26**, 492201 (2014).
 - ²⁶ E. de Mello and J. Sonier, Phys. Rev. B **95**, 184520 (2017).
 - ²⁷ E. V. L. de Mello, J. of Phys.: Cond. Matter **33**, 145503 (2021).
 - ²⁸ H. S. Santana and E. de Mello, Phys. Rev. B **105**, 134513 (2022).
 - ²⁹ H. Santana and E. V. L. de Mello, Phys. Rev. B **107**, 184514 (2023).
 - ³⁰ A. Kanigel, U. Chatterjee, M. Randeria, M. R. Norman, G. Koren, K. Kadowaki, and J. C. Campuzano, Phys. Rev. Lett. **101**, 137002 (2008).
 - ³¹ S. Ono, S. Komiya, and Y. Ando, Phys. Rev. B **75**, 024515 (2007).
 - ³² T. Yoshida, M. Hashimoto, I. M. Vishik, Z.-X. Shen, and A. Fujimori, J. Phys. Soc. Japan **81**, 011006 (2012).
 - ³³ T. Kondo, W. Malaeb, Y. Ishida, T. Sasagawa, H. Sakamoto, T. Takeuchi, T. Tohyama, and S. Shin, Nature Communications **6**, 7699 (2015).
 - ³⁴ Y. Ando, Y. Kurita, S. Komiya, S. Ono, and K. Segawa, Phys. Rev. Lett. **92**, 197001 (2004).
 - ³⁵ I. Tsukada and S. Ono, Phys. Rev. B **74**, 134508 (2006).
 - ³⁶ E. V. de Mello, J. Phys.: Condens. Matter **32**, 40LT02 (2020).
 - ³⁷ E. de Mello, J. Phys.: Condens. Matter **32**, 38LT01 (2020).
 - ³⁸ E. V. L. de Mello and R. B. Kasal, Physica C: Superconductivity **472**, 60 (2012).
 - ³⁹ K. K. Gomes, A. N. Pasupathy, A. Pushp, S. Ono, Y. Ando, and A. Yazdani, Nature **447**, 569 (2007).
 - ⁴⁰ T. Shibauchi, H. Kitano, K. Uchinokura, A. Maeda, T. Kimura, and K. Kishio, Phys. Rev. Lett. **72**, 2263 (1994).
 - ⁴¹ S. Gasiorowicz, “Quantum physics,” (John Wiley and Sons, Inc., New York, 1974).